Article:

Jia, X and Garboczi, E (2016) Advances in shape measurement in the digital world. Particuology, 26. pp. 19-31. ISSN 1674-2001

https://doi.org/10.1016/j.partic.2015.12.005

Review article for Particuology (November 9, 2015)

Advances in shape measurement in the digital world

Xiaodong Jia[*1] and Edward J Garboczi[2]

[1] School of Chemical and Process Engineering, University of Leeds, Leeds LS2 9JT, UK

[2] Material Measurement Laboratory, National Institute of Standards and Technology, Boulder, CO 80305, USA

* Corresponding author: x.jia@leeds.ac.uk

Abstract

The importance of particle shape in affecting the behaviour of powders and other particulate systems has long been recognised, but until fairly recently particle shape information has been rather difficult to obtain and use compared to its more well-known companion - particle size. Because of advances in computing power and 3D image acquisition and analysis techniques, the measurement, description and application of particle shape has experienced a great leap forward in recent years. Since we are in a digital era, it is befitting that many of these advanced techniques are digitally based. This review article aims to trace the development of these new techniques, highlight their contributions to both academic and practical applications, and present a future perspective.

Keywords: particle shape; digital methods; review; shape measurement; spherical harmonics; X-ray tomography

1. Introduction

Everyone whose job involves dealing with particles probably agrees that particle size is one of the most important parameters characterising particles. Many also appreciate that, for non-spherical particles, there is no such thing as "the" particle size, since the so-called size may have many different values depending on the method of measurement, definition of “size,” and the purpose of the “size” determination (Jennings and Parslow, 1988; Allen, 2003). This is all because of particle shape. Non-spherical particles do not have the isotropy of a sphere, meaning the result of even a direct measurement of its linear dimension may vary with the direction of measurement. Think about a pebble being measured with a ruler by hand or virtually in a computer. Results from indirect measurements (e.g., by light scattering or sedimentation) are different even for spheres (Andrès et al, 1996; Allen, 2003), let alone non-spherical particles (Black et al, 1996; Mühlenweg and Hirleman, 1998; Naito et al, 1998; Walther, 2003; Xu and Di Guida, 2003; Eshel et al, 2004; Blott and Pye, 2006; Xu, 2006; Agrawal et al, 2008; Tinke et al, 2008; DiStefano et al, 2010; Califice et al, 2013).

In theory, particle shape can be as important as particle size for the characterization of particles for various applications. For example, many physical properties of powders, including effective conductivity, mechanical strength, and flowability, depend on contact characteristics between the particles. Regardless of size, contact characteristics between spheres are very different from those between non-spherical particles. Spheres have only point contacts. Although in reality such point contacts do have a finite size (contact area and depth), their size and distribution around spherical particles are comparatively much more uniform than for non-spherical particles. Non-spherical particles can have area (face) and line (edge) contacts as well as point contacts. Considering the mechanisms underlying the properties such as shear resistance, flowability, electrical, and thermal conductivity, it should be obvious that particle contact characteristics have a profound influence on these powder properties.

In practice, the effects of particle shape on powder properties and behaviour have been reported numerous times (Meloy, 1977a and b; Swanson and Vetter, 1985; Dixon, 1988; Kaye, 1997; Santamarina and Cho, 2004; Cho et al, 2006). Some will be briefly described in a later section; below are but a few illustrative examples. The Brazil nut effect in particle mixture segregation is well known, and size difference is regarded as the key factor (Williams, 1976; Möbius et al, 2001). However, when different shapes are mixed, segregation can take place even when particles have the same ‘size’ by some measure. The experiments by Ramaioli et al (2005) demonstrate the point well. Three shapes of equal volume (i.e., S = Spheres, SS = Short Sphero-cylinders and LS = Long Sphero-cylinders) are used to form three binary mixtures. After 20 minutes of vibration, all three mixtures showed clear segregation. As illustrated in Fig.1, SS tend to stay on top with a random orientation; LS at the bottom and mostly oriented vertically. The S-SS case may be as expected since the SS appear larger to the eye, and larger particles are expected to come on top in a typical Brazil nut effect. However, in the S-LS and SS-LS cases, the reverse is happening. In the pharmaceutical industry, in an attempt to minimise segregation in blending operations, a common practice is to use the same or similar sized particulate ingredients. However, segregation is still a problem in these operations (Shah et al, 2007; Cullen et al, 2015) and particle shape difference is often blamed. A simple, geometric explanation, by Caulkin et al (2010), is that segregation is a result of different relative mobility determined by particles having different coordination numbers due to their size and/or shape differences while in relative motion. According to a dissolution model by Jia and Williams (2007), for dissolution of solids, particle shape (if they are standalone) or granular structure (if they form agglomerates) determines the relative rates of dissolution, and the ranking is not affected by stirring (which merely shortens the dissolution time). Since dissolution takes place at the particle surface, the surface-area-to-volume ratio must be behind this behaviour, and the value of this ratio is sensitively dependent on particle shape, with a minimum value of this ratio being obtained by spheres (Pólya and Szegö, 1951).

Fig.1 Segmentation example

Given the inherent and intricate links between particle size and shape, it is only fair to say that where size matters, shape does, too. The influence of particle shape on powder material properties and behaviour has long been recognised (Gray, 1968; Chow, 1980; German, 1989; Cumberland and Crawford, 1987; Seville et al, 1997; Allen, 2003), but until fairly recently (over the past 15 years or so), because of the difficulties associated with measurement and description of shape, little could be done to acquire and utilise shape information. In the 1990 edition of the now classic textbook on particle sizing by T Allen (1990), only 16 out of the 800+ pages were devoted to particle shape. In another authoritative book, the 1997 edition of Powder Technology Handbook (Gotoh et al, 1997), the situation was similar: only 13 out of 900+ pages were about particle shape.

Shape is usually described by a combination of qualitative and quantitative descriptors. The former help the reader to mentally visualise the shape; the latter are used for comparisons and calculations. Depending on purpose or application, quantitative descriptors, or shape quantifiers, are classified into three categories. Shape coefficients are typically used to link particle size to its volume or surface area. Shape factors are dimensionless scalars and typically used to quantify a single aspect of the shape. Shape indices are size ratios or shape factor ratios proposed specifically to link particle shape to some shape related properties (Tsubaki and Jimbo, 1979a and 1979b; Sastry et al, 1997). In addition to single scalars, parametric sets can be used to reconstruct shapes. Depending on the method of measurement, shape descriptors can also be classified as geometric or dynamic.

In this review article, the focus will be on advances in shape measurement, shape description and use of shape information in the digital world, since the majority of noteworthy advances in the field rely on, and output results in the form of, digital images. Thus, this review precludes sizing techniques that can also be useful for quantifying shapes, such as sieving (Persson, 1998) and angle of repose (Friedman and Robinson, 2002); and dynamic techniques based on, for instance, measurements of settling speed (Krumbein, 1941; Medalia, 1970; Black and McQuay, 2001) or conductivity (Furuuchi et al, 1988). A recent review by Rodriguez et al (2013) covers some of these. The present review puts the emphasis on providing commentary on the status quo, potential applications, and future prospective, rather than an exhaustive textbook-style summary. For applications, the emphasis will be on the so-called digital approach, which is also referred to as the lattice approach, the pixel-based (2D) or voxel-based (3D) approach, or the pixelated or voxelated approach.

The paper is divided into three main sections: measurement, description and use. The paper will conclude with a brief summary and future perspectives.

2. Shape measurement

Demands for shape analysis, and hence shape measurement, generally come from the following areas (some specific examples are given in Section 4):

- From industry, for quality assurance or control. For such purposes, it is desirable to use as few parameters as possible, especially if the control is online. Here the focus is on how particle shape affects final product properties. The aim is to establish and use a definitive correlation between product quality and certain shape descriptors. Although helpful, the relationship need not be a cause-and-effect one. Such requirements can usually be met by one or at most a few shape factors.
- From researchers in both academia and industry, for better understanding of a particular phenomenon or for better powder formulation. In these situations, the focus is on why the particle shape matters to final properties. The aim is to establish causality; but again it is desirable that as few shape descriptors are used as possible.
- From computer modellers doing particle-level simulations, often called discrete element method (DEM) simulations (Radjaï and Dubois, 2011). In such simulations, particles are represented, stored and manipulated individually, so that shape factors or ratios alone are no longer sufficient or even useful. The focus now is on re-creation of the individual shapes and any shape factor/ratio will have already been embedded in reconstructed shapes. For such applications, real-time digitisation would be ideal, but in reality this is a bottleneck and the most time consuming part of non-spherical simulation exercises.

As far as shape measurement is concerned, two advances are noteworthy and reviewed here. One is the gradual transition from 2D to 3D, and the other has to do with new image processing techniques for shape extraction or quantification. For measurement, both hardware and software are important; therefore they are reviewed together.

2.1 2D measurements

Traditionally, shape measurement and analysis were performed on the physical objects directly or on photographs or micrographs. Either way, it was largely a manual, painstaking, error-prone and time consuming task. Today, a small number of large objects may still be measured this way, but the majority of 2D shape measurement and analysis is now carried out by a computer, using digital images of the objects. This advance has meant increased speed, accuracy, availability, and number of measurable shape factors, thereby paving the way for wider utilisation of shape information.

As will be seen later, most shape factors in use today are defined in terms of quantities obtained from 2D projections of particles. Current industrial practice in quality assurance or control is established based on these shape factors - if particle shape is even considered in the first place. This is because, traditionally, 2D images were the only images readily available for use. Partly limited by computing power, and partly due to this common practice, most commercial shape analysers available today are designed to use 2D projections of images for shape as well as size measurements. Although fast and inexpensive, quantifying shapes of real (3D) particles using their 2D projections has some obvious problems.

Figure 2: Cylinder and its 2D projections.

The problems can be illustrated with the help of Figure 2, which shows a cylinder and its 2D projections. Except for the rare cases where the projections are known to come from a single object or objects of an identical shape, there is always a danger (or one might say the inevitability) that the cylinder be misrecognised as a sphere, a disc, a rectangular plate, a cube, or a spherocylinder. When these projections are used to calculate a shape factor, instead of a single value true to the cylinder, a distribution is likely to be the result. When these projections are used for sizing, a bimodal size distribution is usually obtained, with one peak corresponding to the length and the other to the diameter of the cylinder. Exact calculations have been carried out for tri-axial ellipsoids, where the 2D projections are always ellipses but of varying aspect ratios (Gendzwill and Stauffer, 1981; Vickers, 1996).

Given a 2D image (e.g., a projection) of a particle, the most common treatment is to make it binary (if not already so) then use its area and/or its perimeter for size and shape analysis (Pons et al, 1999; Pons et al, 2002). For binary digital images, there is no ambiguity in area, which is equal to the number of solid pixels; but perimeter is another matter. Imagine a line segment parallel to the X axis that is 100 pixels long. If the line segment is 45 degrees to the X axis, the pixel count becomes 72. This is still a perfect case for correction since all pixels are in point contact with one another, and each now has a length of exactly $\sqrt{2}$, so the total length is $72\sqrt{2} = 101.8$ or only 1.8 % longer than reality. For any other angles between 0 and 90^{o} the error is likely to be greater, even with special corrective measures such as chain-coding (Yang et al, 1994; Russ, 1995). Compounded to this is a more subtle, and harder to quantify, source of error: the original line segment may have been a straight line segment of the given pixels only at this particular resolution, with finer details lost. Thus, it is worth bearing in mind that, although use of perimeter allows more shape factors to be computed, they also contain more uncertainty (Schäfer, 2002; Zeidan et al, 2007) than those factors based only on area. The accuracy may be improved by increasing the resolution, but digitisation errors always exist and the improvement is not a monotonic one but a oscillating one. Consider the digital representation of a circle. If digitisation error is defined as the relative difference in area between the digital shape and the ideal continuum shape, the errors corresponding to circle diameters of 6, 7, 8, 10, 16, 17 and 18 pixels are 13.2 %, -3.9 %, 3.5 %, 1.9 %, 3.5 %, -0.9 % and 0.6 %, respectively.

Even just for geometric description, the number of shape factors is large compared to that of the more standardised 'sizes'; but in terms of usage, they all fall into one of three categories: those that describe how close a shape is to an ideal (e.g., sphericity or circularity); those that describe at a high level the form or curvature (e.g., roundness, aspect ratio); and those that describe surface roughness or texture (e.g., asperity, angularity). Mora and Kwan (2000) have provided a review of shape analysis based on digital image analysis. Their review is still current, with only one additional point to be added below.

Sometimes 2D images containing textural information of the particles are obtained from photographic imaging, as in scanning electron microscopy (SEM) and transmission electron microscopy (TEM). However, they are generally turned into binary images and used as if they were 2D projections. Only a tiny fraction of the information contained in an image is actually used, since the vast majority of information, in the form of shades and texture, is simply discarded.

Figure 3: Diffraction pattern of a circle and a square. SEM photo of particles with texture information.

Use of laser diffraction patterns to obtain particle shape information was proposed by the late Professor Brian Scarlett and his team (Ma et al, 2000, 2001a and 2001b), but the research does not appear to have continued, except for a few special cases (Deriemaeker and Finsy, 2005). As Figure 3 shows, shape information is clearly embedded in the diffraction patterns (Figure 3a) or in the shades or textures in photo/SEM images (Figure 3b). For diffraction patterns (Figure 3a), currently the size and distance of the light blobs are used to extract size information; the rest is discarded. For photo images (Figure 3b), only the edges are used to obtain size information and sometimes shape factors based on 2D projection areas. The difficulty associated with this line of attack is similar to that faced by computer scientists attempting to make use of texture/shading information contained in normal or SEM images. In both cases, shape information is embedded in the image, but the texture/shading information is currently simply discarded. Shape reconstruction from images of shapes or scenes is an active research area, but its application to particle size/shape measurement may be still years away. 3D facial reconstruction from a single image (e.g., Kemelmacher-Shlizerman and Basri, 2011) and automatic facelift of photo portraiture are already a reality. This is because although faces vary from person to person, all normal human faces share enough common features for a generalised template matching approach to be feasible. By comparison, variation in size and shape among powder particles can be orders of magnitude greater; as is the level of difficulty in dealing with such large variations.

2.2 2.5D measurements

Between the 2D and full 3D measurements lie what may be called 2.5D techniques. They are generally based on the merging of a small number of 2D images, not enough so as to form full 3D shapes, but still yielding shape information that is more complete than from single 2D images/projections. These mainly optically-based techniques do not image the dark side of illuminated particles, hence categorizing them as 2.5D rather than 3D techniques.

Confocal optical microscopy (or confocal laser scanning microscopy) is a useful tool for observing small (colloidal) particles in suspension or at rest. If images of stationary particles from different focal depths are stacked together to form a volume, it is possible to extract shapes from the stacking. It is worth noting that depth resolution may be different from lateral resolution, and some corrective measures will be necessary during stacking or during analysis to ensure shapes are not distorted. For practical applications, this method is subject to the same constraints as normal optical microscopy in the two lateral directions, and additionally also to depth resolution and confocal range in the third (vertical) direction. McCormick and Gee (2005) demonstrated its use for shape analysis of some abrasive particles. In a more recent example, it was used to characterise contacts between primary particles in colloidal aggregates (Wang et al, 2012).

Closely related to confocal microscopy is 3D surface profilometry. It is designed to examine dry and static objects/surfaces and is able to scan a much larger volume with a finer resolution than confocal microscopy. Focus-stacking is popular among photo enthusiasts as a way to extend depth of field. With this technique, images taken at gradually incrementing focal distances across the object are merged to form a final image with every part pin-sharp. In principle, it is similar to the confocal technique. Although not yet seen in practical use, it is theoretically possible to make use of the depth information and narrow focal depth in each image to reconstruct 3D shapes out of a stack of images.

The digital elevation method operates at the other extreme of the length scale. It is typically used for geo-sized landscape survey; but as in the above techniques, surface topology is obtained from distance mapping of surface contours.

Using SEM stereo imaging, also called stereomicroscopy, it is possible to reconstruct 3D surfaces at the micrometer size level (Pouchou et al, 2002; Mills and Rose, 2010; Roy et al, 2012), and it can cover more depth and wider area than AFM (atomic force microscopy) for the same purpose (Vickerman and Gilmore, 2009). Although primarily for surface roughness analysis, it should be easy to make use of the information for shape analysis of particles if they are in the right size range; i.e., close to the roughness height that the equipment is designed to measure.

However, all the above techniques have the same major deficiency for 3D shape measurement: they only give half the 3D object, the upper, “illuminated” half.

2.3 3D measurement

For shape characterisation of real particles, nothing compares with full 3D imaging. Digitisation errors aside, a full 3D virtual shape is better than a physical one since more shape quantities can be calculated by a computer on the virtual shape than can be measured by hand on a physical object. Equipment that can be used for 3D shape reconstruction and analysis have existed for some time, but they are generally not designed or made for this purpose. As a result, the level of automation in shape analysis by software is much lower than that for 2D images, and the main use of 3D imagining devices has been to digitise the particles in 3D. It is then up to the users to perform shape analysis one way or another (frequently by in-house software programs); and there is no standardisation in procedure and reporting as there are for 2D measurements.

The greatest advance in this area has to be X-ray computed tomography (CT). X-ray micro CT scanners for material characterisation operate on the same principle (Herman, 2009) as medical CT scanners in hospitals, only with 1000x better resolution (i.e., micrometer spatial resolution compared to millimeter spatial resolution) for a fraction of the price. A decade ago, a desktop CT scanner was a rarity even in large, research intensive universities. Now, it is common for a large university to have more than one CT scanner.

Use of X-ray techniques for particle size measurement started as early as 1937 (Jones, 1938). Today it has become a favourite tool for digitising hard-to-describe 3D shapes such as sand grains, agglomerates from granulation process, or broken ore particles from crushing or grinding. For particle sizing, a rule of thumb for particle projection images to be counted for analysis is that the image should be at least 5 pixels across. In CT scan volume, a similar rule of thumb exists (but may vary from one operator to another and/or from one shape to another). To have any confidence in resolving a shape, it should be at least 5-10 voxels across (Garboczi, 2002). Given that most so-called high-resolution or micro CT scanners have a practical resolution limit of 1 micrometer per voxel, even under ideal conditions, particles less than ~10 micrometers are difficult to analyse by CT scanning, especially if they are packed together (as in a powder sample). For very carefully prepared samples on some machines, voxel sizes of about 0.4 micrometers have been achieved, allowing for 4 µm particles to be analysed in 3D (Cepuritis et al, 2015).

A CT image can be regarded as a mass density mapping of the sample. In many cases (e.g., Williams and Jia, 2003; Baker et al, 2012; Cnudde and Boone, 2013), features to be distinguished have sufficient contrast from the background and/or from each other, so that simple thresholding can separate them. If features of interest or components have close density values and thus look the same or similar in greyscale CT images, a more sophisticated method of separation is required. The most popular one is the calibration method as it does not require measurement by another technique, so is more convenient, cheaper and faster. A recent example is given by Pankhurst et al (2014) for volcanically formed crystals of different chemical compositions. Another possibility (Jia and Williams, 2007) would be to merge data from chemical imaging (Kazarian and Chan, 2003; Ma and Anderson, 2008; Kazarian and Ewing, 2013) with CT scan data for cases like dissolution of tablets. However, since chemical imaging usually only works on surfaces, only the surface slice can possibly be data fused this way; and so far it remains only a possibility. Cordes et al (2014) described a method whereby a CT scan was combined with X-ray florescence spectroscopy to provide added contrast for components containing different metallic elements. The possibility of combining mineral stereological information with CT images was raised for application in a leaching simulation (Jia et al, 2008); it is now a commercial reality that 3D CT can be merged with SEM to provide "true 3D microscopy" at sub-micrometer resolutions (e.g., Bruker, 2015; Miller et al, 2012).

Real-time CT scan and reconstruction for medical and industrial use is not only a technological feasibility but is already a commercial reality (Sacca, 2015). However, such equipment is currently limited to relatively large objects (cm sized or above), perhaps too large for most particle technologists, and the cost is prohibitive to most (much higher than the already rather expensive desktop CT scanners). If the commercial drive is strong enough, cheaper and wider availability can be expected. GPU reconstruction is also being offered by some scanner manufacturers and third-party vendors, with 10x or more speedups achieved compared to CPU reconstruction.

Along with CT scanning, another digitisation technique which has seen rapid advances in recent years is 3D optical scanning (Curless and Levoy, 1996; Chen et al, 2000; Zhang et al, 2010; Chandra Pati, 2012). As with any new technology, it has followed the usual trends such as increasing resolution and speed while reducing price, and the ability to work in ambient light, as opposed to a dark room environment, is no longer necessary. Compared to CT scanning, it is advantageous in terms of cost (US $K vs US $100K), speed (minutes vs hours) and ease of use. Its limitations are also obvious, including restriction to convex shapes in general, surface digitisation only, and low resolution (0.1 mm vs 0.5 um). The point cloud obtained from optical scanning is normally converted into a surface mesh for output, thus an extra back-conversion step is needed if volumetric data form is required, unless the original point cloud can be made available to equipment users. With a CT scan, the material or component distribution inside the body of the 3D objects is readily available, at the voxel level, for structure-property relationship calculations (e.g., conductivity). With surface meshed objects, internal structural heterogeneity must be obtained and specified in some other way.

Nowadays CAD tools can as a matter of course provide 3D renderings of mechanical designs. This is in addition to the traditional three orthogonal projections that are typically used to represent 3D objects. The reverse is the idea behind 3D shape reconstruction from three orthogonal shadow images (i.e., projections) (Bujak and Bottlinger, 2008). The reconstructed shape may be inaccurate for some applications but better than 2D measurements in determining shape factors (Kuo et al, 1996). Working with only a few projections, instead of 100s to 1000s as in CT scanning, has the obvious advantages in speed and cost, but also some obvious deficiencies in accuracy and shape restrictions.

All the above 3D shape measurement techniques work on a prerequisite that the projections are from known angles. What if they are not? Projections from many existing particle size/shape analysers are abundantly available. They are from particles at unknown (or random) orientations, but successive projections may be expected to have tractable correlations. If such correlations can be utilised, with some restrictions and with the help of some a prior knowledge and GPU processing power, it is in theory possible to reconstruct shapes from projections of unknown directions. Some developmental work has been done in this area (e.g., Laurentini, 1997; Liang and Wong, 2010), but further work is required for practical use.

2.4 Shape identification and extraction by software

2D commercial size/shape analysers are usually bundled with special dispersion mechanisms and/or procedures to help ensure particles are well separated in the images collected by the hardware. The number of uncertain situations (e.g., due to actual and suspected overlaps) is relative small, and can afford to be simply discarded. It is then a relatively easy job to analyse individual particles projections to obtain shape factor statistics.

However, when using non-purpose built equipment (e.g., SEM and CT) for shape measurement, including in-situ imaging of processes where it is impractical to implement or install a dispersion mechanism to ensure particle separation in images, either particles must stay separated in the physical sample or segmentation must be carried out on the images. Either way is a time-consuming process. To analyse a given number of particles, in the case of SEM images, time is mostly spent on imagining since multiple scans are required; in the X-ray CT case, time is mostly spent on identifying and extracting the particles through a process called segmentation. The former is hardware bounded and costly; the latter relies on software capability or end users' patience and is generally regarded as a cheaper and hence more attractive option. Therefore, development and implementation of segmentation algorithms are critical to the success of the second option mentioned above (see also Figure 4a for example). Advances in this respect include increasing ability to handle less favourable situations (e.g. particles that are not well-separated) (De Anda et al, 2005; Karakuş et al, 2010), capability to deal with 3D volumes directly (Videla et al, 2006; Whitmarsh et al, 2011; Roberts et al, 2012), and automation of the procedure with little loss of accuracy compared to manual separation (Long et al, 2007). Popular software packages that have such capabilities include the open-source 3D ImageJ Suite for 3D watershed segmentation and 3D analysis (Ollion et al, 2013) and various commercial options. In favourable conditions, what used to be days of hard labour can now be reduced to a few mouse clicks and minutes of machine time!

If particle shape is known, but extraction of the shape is required for other analyses (e.g., orientation distribution of certain shape in a packing, as in Figure 4b), a Markov-chain Monte Carlo template matching technique may be used (Caulkin et al, 2009). In packing of multiple shapes, template matching may be performed multiple times, each targeted at a particular shape.

Figure 4: Example of CT scans of packing and extraction of particles.

3. Shape description

Shape is normally described by a combination of qualitative and quantitative descriptors. Qualitative descriptors are words, often adjectives, like spherical, rounded, fibrous, flaky, irregular, angular and acicular, tabular, equant, lamellar, columnar, isometric, tetragonal, or hexagonal. For historical reasons, different disciplines have developed and used their own glossaries. For example, a "plate" to a powder handler may be called "isometric lamellar" by a pharmaceutical worker. Within a discipline, standards do exist. Examples of national, international and professional body standards include: BS 2955:1993; USP24; ASTM F1877-98; ISO 9276-6:2008, and NIST Glossary of Morphology Terms.

While qualitative descriptors help the reader to mentally visualise the shape, quantitative descriptors are used for comparisons and calculations. Even by a rough count, there are close to 100 different shape descriptors, describing all conceivable aspects of particle shapes. They describe either geometric (static) or dynamic attributes of shapes; and are either single-parameter scalars or parameter sets, as briefly described below. Among the single-parameter scalars, a distinction can be made between coefficients (used to relate particle size to volume or surface area), factors (dimensionless quantities used to describe some aspects of shape) and indices (ratios designed for specific purposes). For convenience, they are simply referred to as 'shape factors' in the following discussion, unless a finer distinction is necessary.

3.1 Single factors

Most shape factors used today in particle technology originated from other disciplines, notably from geologists (Wentworth, 1922 and 1933; Wadell, 1932, 1933, 1934 and 1935; Heywood, 1937; Krumbein, 1934 and 1941; Barrett, 1980) and computer scientists (Russ, 1995; Costa and Cesar, 2001; Zhang and Lu, 2004; Tangelder and Veltkamp, 2008; Kazmi et al, 2013). Geologists needed to have a measure of shape for their rocks and pebbles, which tend to be large enough to be measured by hand. Computer scientists were interested in ways to accurately represent or recover shape with as few parameters as possible. A commonality between the two groups is that, whether physical or virtual, the objects they have to measure can be manipulated almost at will, and their shape descriptors have a relatively straightforward link to the effects that the shape descriptors were invented to describe. Particle technologists and practitioners did not have that kind of luxury, for two notable reasons. First, until recently (or even now), particle technology has never been a subject area in its own right. People invented and re-invented what was suitable for their own needs in their own fields using their own customary measurement methods and techniques. Consequently, there is a lack of common standards and no concerted effort for standardisation of shape descriptors. Second, the objects to be measured are typically too small to see or manipulate easily, and too many to quantify by hand. This necessarily limits the types and numbers of measurements that can be routinely applied. Also, the link between shape and known phenomena can be hidden behind size effects.

Shape factors are generally used to describe one of three types of attributes: closeness to an ideal shape (sphericity); curvature of the overall form (roundness); and details of surface texture (asperity). They have received several reviews over the years (Clark, 1987; Pons et al, 1997; Mikli et al, 2001; Muller et al, 2001; Faria et al, 2003; Pourghahramani & Forssberg, 2005). The general trends may be summarised as: from simple to complex, 2D to 3D, overall to detail, and manual to automatic. For example, the concept of fractal dimensions has been adopted for describing agglomerates, starting with analysis of their 2D images (Kaye, 1978, 1994 and 1997), moving up to 3D flocs largely with the help of computer models (e.g., Witten and Sander, 1981; Shih et al, 1991; Jia et al, 2000), extending to faceted 3D objects (Pons et al, 1998), becoming automated (Wettimuny and Penumadu, 2003) and measurable by other means such as different kinds of small angle scattering (Schaefer et al, 1984; Beaucage, 1996; Bushella et al, 2002).

The prevalence of images and image analysis techniques means that it has become much easier to define and use one's own shape factors in pursuit of a link between shape and powder behaviour. The number of factors defined and explored may be increasing, but fundamentally there are not many advances in this area. It is generally advisable (Hentschel and Page, 2003) to use two descriptors, one for the overall form and one for surface texture details.

3.2 Parametric series

Mathematically, it is possible to represent any smooth curve outline of a particle using a harmonic series. If a particle shape profile can be expanded into a distance (r) vs angle (ϕ) curve (Figure 5a), it can be represented in the same way. This is the basic idea behind harmonic analysis of shapes (Kaye, 1999). For profiles containing re-entrants, the distance (r) may not be unique for a given angle (ϕ) (Figure 5b). For such cases, a complex Fourier series can be used (Schwarcz and Shane, 1969; Gotoh and Finney, 1975; Meloy, 1977a and 1977b; Clark, 1981; Bowman et al, 2001). In complex Fourier analysis, the profile is circumnavigated in the complex plane at a constant angular speed chosen such that one circumnavigation takes 2π time and 2^m steps. Depending on how many descriptors are retained in the series, shape can be recovered with various degrees of accuracy. The first few descriptors correspond to some familiar quantities: radius (0), elongation (-1), triangularity (-2), squareness (-3) and asymmetry or irregularity (+1). With 3D shapes becoming available for analysis, 3D Fourier shape analysis can also been performed (Vranic, 2001). However, it can become increasingly cumbersome as the shape becomes rougher or more angular, since the number of descriptors required can easily go beyond 100. For faceted particle shapes, polygonal harmonics are a more natural choice (Young et al, 1990; Pons et al, 1998).

Figure 5: Fourier analysis of shapes.

Figure 6: Shapes generated by spherical harmonics.

For star-shaped particles, covering particles typically found in cement and concrete, in mineral and metallurgical processes, 3D printing and even for simulated lunar soil, spherical harmonic analysis has been developed (Garboczi, 2002 and 2011; Garboczi and Bullard, 2016; Slotwinski et al, 2014). A particle is convex if the line segment connecting any two points chosen in the particle or on the particle surface also lies in the particle. A star-shaped particle is similar, but one of the two points is fixed. If the line segment connecting this special point with any other point in the particle is also contained in the particle, then the particle is star-shaped (Ritchie and Kemp, 1999). If a particle is star-shaped, then using the one special point as the origin, the surface of the particle, denoted by $r(\theta,\phi)$, where $r(\theta,\phi)$ is the distance to the particle's surface in the direction given by the two spherical polar angles, can be expanded in spherical harmonic functions (Fig.6a). The coefficients of the expansion then contain all the size and shape information for the particle available in the original particle image.

To characterize the shape of a powder, samples are prepared consisting of particles dispersed in epoxy, then sucked by vacuum into a plastic tube (Erdoğan et al, 2006). The hardened sample is imaged in the X-ray CT, the resulting images are thresholded, and special software extracts the particles and fits them with a spherical harmonic series (Fig.6b). The random-shaped particle is now completely mathematically described, up to the imaging voxel size, and any shape coefficient, factor, or index can be easily calculated. As well, 2D projections in any direction can be made so as to quantitatively compare to the results from 2D particle shape analysis instruments (Cepuritis et al, 2015). There have been many applications of this joint X-ray CT and spherical harmonic analysis to many different materials (Garboczi and Bullard, 2016). Particle-particle contact can also be determined using these techniques (Garboczi and Bullard, 2013), and new particles can be mathematically generated, which are statistically similar to real particles that have been previously characterized (Grigoriu et al, 2006; Liu et al, 2011). Also, it was mentioned above about the intertwining of particle size and shape – measurements of size, even for a technique as simple as a sieve analysis, depend on the shape of the particles considered. Comparison of sieve analysis, laser diffraction, and spherical harmonics has been carried out illustrating this mutual dependence (Erdoğan et al, 2007).

One possible drawback of the spherical harmonic analysis is dealing with mathematical artifacts in the spherical harmonic series. A well-known artifact introduced by truncated SH series representations is the Gibbs phenomenon, or "ringing"—the appearance of small, high-frequency ripples on the surface and especially near the poles. However, a common technique for reducing the ringing artifact, without significantly affecting the overall shape, is to filter the series with the so-called Lanczos sigma factor (Bullard and Garboczi, 2013; Lanczos, 1956) at the probable price of removing some real surface detail along with ringing artifacts.

Having a coherent set of parameters to give an analytical approximation of real particle shapes, or to simultaneously describe multiple attributes of a whole class of shapes, is a powerful tool. It is easier to calculate any shape functional, including all the shape factors, for these approximations than for the real particles (physical or digitised). Shapes and their differences can now be quantified more meaningfully than by a single shape factor, for particles within a powder or for different powders (Raj and Cannon, 1999). It also makes it possible to easily retrieve and compare finer features among shapes (Zhang and Lu, 2004).

It is also envisaged that parameterisation of complex shapes can make it easier for particle extraction from CT scans of packing by template matching; for shape generation for particle level simulations; and for model based tomographic reconstructions.

3.3 Shape presentations and representations

Like particle size, shape factors are often plotted against another property of interest to show the correlations between the two. Some graphical charting schemes (Davies, 1975; Tsubaki and Jimbo, 1979b; Benn and Ballantyne, 1993) have been proposed to visually differentiate shapes of particles from the same original powder. In such maps, shape factors are plotted against each other or against a size, but not against a physical property of interest. A tri-plot example is given by Graham and Midgley (2000), where shapes ranging from blocky to oblate or prolate can be mapped linearly along the scales. Kaye et al (1998) also used 3D plots involving fractal dimension, chunkiness and size, so that particles of different size and shape characteristics form different groups in the plot, which are immediately apparent to the reader.

For applications such as computer graphics and particle level computer simulations, shape needs to be represented individually for display and manipulation. Broadly, there are four types of shape representations in use: three are vector based and one digital, as summarised in Table 1 below. Commercial software packages are available to convert between the different forms.

Table 1: Comparison between shape representations typically used in particle simulations

4. Use of shape info

The majority of the devices used today for shape measurement and digitisation were not originally designed for such purposes. Shape analysis was an add-on feature to existing imaging-based particle size analysers, using the same data (i.e., projections) that were collected for sizing. In this sense, users have largely been the beneficiary rather than the driving force behind many of the hardware capability enhancements that we have seen. On the other hand, users have been inventing and reinventing shape descriptors for their own purposes all along; but only a selected few are adopted by commercial shape analysers. Regardless of this apparent disparity between shape measurement and shape description, without applications, there would be no market and little commercial incentive for a sustained future development beyond the initial add-ons.

Applications of shape information may be divided into two main groups: passive and proactive. In a passive use, shape information is collected to help explain puzzling observations in practical situations or for product quality control. In a proactive use, particle shape information is treated as a variable and used to inform purposeful changes in powder formulation and product design.

Examples of passive use, in the form of observed shape effects in packing, segregation, powder blending and dissolution, have been mentioned earlier in this paper. More examples can be cited, including effects of particle shape on conductivity (Friedman and Robinson, 2002) and avalanching (Robinson and Friedman, 2002) of granular media; on filtration rate (Connell et al, 1999); on tensile strength (Mirghasemi et al, 2002); on product quality (De Anda et al, 2005); and a wide range of properties of cement and aggregates (Garboczi and Bullard, 2016) and geomaterials (Alshibli and Reed, 2010).

Compared to passive use, there are relatively few examples of proactive use of shape, especially if those already used for shape measurement (Furuuchi et al, 1988) are excluded. One notable example is the use of shape as an additional parameter for design of micro- and nano-scale drug delivery carriers (Champion et al, 2007) and control of formation of nanocrystals (Paik et al, 2015).

Computer models, particularly those that are designed to handle different particle shapes, can be used for both passive and proactive applications. One example is optimisation of geometry of pellets used in packed column reactors (Caulkin et al, 2009). To be cost effective and time efficient, such uses usually require that the link between shape and quality, by whatever measure is used, is known or can be established by computer models rather than having to rely on making and testing new physical shapes. Proactive use of shape information can be expected to see a more rapid increase now that the enabling tools, both measurement hardware and simulation software, are emerging and becoming readily available.

5. Concluding remarks

For shape measurement, traditional 2D methods are known to be problematic, so 3D methods are preferable. The status quo is an awkward one. 2D methods still play the most important role in practice and are not likely to disappear for the foreseeable future, for economic rather than technological reasons. For computer modelling involving complex shapes, the story is likely to be the same. While the digital approach has a clear advantage (i.e., simplicity) over the vector-based approach, proving its worth against the established methods will be an uphill struggle until the two practical bottlenecks, digitisation of particles and runtime speed, are removed.

In hindsight, the basic ideas behind many new developments were actually available or thought of well before they became practical. It is increased computing power that made possible the advances in shape measurement, description and use reviewed in this paper. If the computing power keeps increasing at the same rate or faster, and assuming computers will remain digital, it should be possible to make some speculations with a fair degree of accuracy on what can happen in the future. Today, vector approaches still have an upper hand over digital approaches in almost every area that matters. Fifty years from now, it may well be the other way around!

Real-time or near real-time digitisation of 3D particles can be expected to be a reality. To a large extent, the basic technologies are already there, ready to be exploited commercially. The speed of commercialization depends more on industrial uptake of shape information than on academic or model requirements. Assuming future computers are still digital, and their power is increasing at the same speed as it has been, it is conceivable that real-time digitisation in full 3D of small particles will be a reality. Simulations based on real 3D shapes at industrially-useful time and length scales are also a possibility.

References

1. T Allen (1990) Particle Size Measurement, 4th Ed, Chapman & Hall.
2. T Allen (2003) Powder Sampling and Particle Size Determination, Elsevier.
3. C Andrès, P Réginault, MH Rochat, B Chaillot, Y Pourcelot (1996) Particle-size distribution of a powder: Comparison of three analytical techniques, International Journal of Pharmaceutics, 144(2): 141–146.
4. YC Agrawal, A Whitmire, OA Mikkelsen, HC Pottsmith (2008) Light scattering by random shaped particles and consequences on measuring suspended sediments by laser diffraction, J Geophys Res, 113: C04023, doi:10.1029/2007JC004403.
5. JC De Anda, XZ Wang, KJ Roberts (2005) Multi-scale segmentation image analysis for the in-process monitoring of particle shape with batch crystallisers, Chemical Engineering Science, 60: 1053–1065.
6. KA Alshibli, AH Reed (2010) Advances in Computed Tomography for Geomaterials: GeoX 2010, John Wiley & Sons, Inc., Hoboken, NJ, USA.
7. DR Baker, L Mancini, M Polacci, MD Higgins, GAR Gualda, RJ Hill, ML Rivers (2012) An introduction to the application of X-ray microtomography to the three-dimensional study of igneous rocks, Lithos, 148: 262–276.
8. PJ Barrett (1980) The shape of rock particles, a critical review, Sedimentology, 27: 291-303.
9. G Beaucage (1996) Small-Angle Scattering from Polymeric Mass Fractals of Arbitrary Mass-Fractal Dimension, J Appl Cryst, 29: 134-146.
10. DL Benn, CK Ballantyne (1993) The description and presentation of particle shape, Earth Surface Processes and Landforms, 18: 665-672.
11. DL Black, MQ McQuay, MP Bonin (1996) Laser-based techniques for particle size measurement: a review of sizing methods and their industrial applications. Prog. Energy Combust. Sci., 22:267-306.
12. DL Black, MQ McQuay (2001) Laser-based particle measurements of spherical and nonspherical particles, International Journal of Multiphase Flow, 27(8):1333–1362.
13. SJ Blott and K Pye (2006) Particle size distribution analysis of sand-sized particles by laser diffraction: an experimental investigation of instrument sensitivity and the effects of particle shape, Sedimentology, 53: 671–685.
14. ET Bowman, K Soga, W Drummond (2001) Particle shape characterisation using Fourier descriptor analysis, Géotechnique, 51: 545-554.
15. DJ Brown, GT Vickers (1998) The use of projected area distribution functions in particle shape measurement, Powder Technology, 98: 250-257.
16. Bruker (2015) True 3D Microscopy for SEM (https://www.bruker.com/products/x-ray-diffraction-and-elemental-analysis/eds-wds-ebsd-sem-micro-xrf-and-sem-micro-ct/micro-ct-for-sem/technical-details.html)
17. B Bujak, M Bottlinger (2008) Three-dimensional measurement of particle shape, Part. Part. Syst. Charact., 25: 293–297.
18. JW Bullard, EJ Garboczi (2013) Defining shape measures for 3D star-shaped particles: Sphericity, roundness, and dimensions, Powder Technology, 249: 241–252.

19. GC Bushella, YD Yan, D Woodfield, J Raperc, R Amala (2002) On techniques for the measurement of the mass fractal dimension of aggregates, Advances in Colloid and Interface Science, 95: 1-50.
20. A Califice, F Michel, G Dislaire, E Pirard (2013) Influence of particle shape on size distribution measurements by 3D and 2D image analyses and laser diffraction, Powder Technology, 237:67-75.
21. R Caulkin, X Jia, C Xu, M Fairweather, RA Williams, H Stitt, M Nijemeisland, S Aferka, M Crine, A Leonard, D Toye and P Marchot (2009) Simulations of structures in packed columns and validation by x-ray tomography, Industrial & Engineering Chemistry Research, 48 (1): 202-213.
22. C Caulkin, X Jia, M Fairweather, RA Williams (2010) Geometric aspects of particle segregation, Physical Review E 81 (5), 051302.
23. R Caulkin, W Tian, M Pasha, A Hassanpour, X Jia (2015) Impact of shape representation schemes used in discrete element modelling of particle packing, Computers & Chemical Engineering, 76: 160-169.
24. R Cepuritis, EJ Garboczi, S Jacobsen (2015) Three dimensional shape analysis of concrete aggregate fines produced by VSI crushing, submitted to Cem. Conc. Composites.
25. JA Champion, YK Katare, S Mitragotri (2007) Particle shape: A new design parameter for micro- and nanoscale drug delivery carriers, Journal of Controlled Release, 121: 3–9.
26. U Chandra Pati (2012) 3D surface Geometry and Reconstruction: Developing Concepts and Applications, IGI Global, ISBN: 1466601132. DOI: 10.4018/978-1-4666-0113-0.
27. F Chen, GM Brown, M Song (2000) Overview of three-dimensional shape measurement using optical methods, Opt. Eng., 39(1):10-22.
28. GC Cho, J Dodds, JC Santamarina (2006) Particle Shape Effects on Packing Density, Stiffness, and Strength: Natural and Crushed Sands, J. Geotech. Geoenviron. Eng., 132:591-602.
29. TS Chow (1980) The effect of particle shape on the mechanical properties of filled polymers, Journal of Materials Science, 15:1873-1888.
30. NN Clark (1987) A new scheme for particle shape characterization based on fractal harmonics and fractal dimensions, Powder Technology, 51: 243-249.
31. V Cnudde, MN Boone (2013) High-resolution X-ray computed tomography in geosciences: A review of the current technology and applications. Earth-Science Reviews, 123: 1-17.
32. H Connell, J Zhu, A Bassi (1999) Effect of particle shape on crossfow filtration flux, Journal of Membrane Science, 153, 121-39.
33. NL Cordes, S Seshadri, GJ Havrilla, BM Patterson, M Feser, X Yuan, Y Gu, D Wang (2014) Subsurface Particle Analysis using X-ray Computed Tomography and Confocal Xray Fluorescence, Microsc. Microanal., 20 (Suppl 3): 778-779.
34. LDF Costa, RM Cesar (2001) Shape Analysis and Classification: Theory and Practice, CRC Press, ISBN: 0-8493-3493-4.
35. PJ Cullen, RJ Romanach, N Abatzoglou, CD Rielly (2015) Pharmaceutical Blending and Mixing, Wiley, ISBN 9780470710555.
36. DJ Cumberland, RJ Crawford (1987) The Packing of Particles, Elsevier, Amsterdam.
37. R Davies (1975) A simple feature-space representation of particle shape, Powder Technology, 12:111-124.

38. B Curless, M Levoy (1996) A volumetric method for building complex models from range images. In Proceedings of SIGGRAPH '96, 303-312.
39. L Deriemaeker, R Finsy (2005) Shape and size determination by laser diffraction: average aspect ratio and size distributions by volume; feasibility of data analysis by neural networks, Part. Part. Syst. Charact., 22:5-13.
40. AG Dixon (1988) Correlations for wall and particle shape effects on fixed bed bulk voidage, The Canadian Journal of Chemical Engineering, 66:705-708.
41. ST Erdoğan, PN Quiroga, DW Fowler, HA Saleh, RA Livingston, EJ Garboczi, PM Ketcham, JG Hagedorn, SG Satterfield (2006) Three-dimensional shape analysis of coarse aggregates: New techniques for and preliminary results on several different coarse aggregates and reference rocks, Cement and Concrete Research, 36: 1619-1627.
42. ST Erdoğan, DW Fowler, EJ Garboczi (2007) Shape and size of microfine aggregates: X-ray microcomputed tomography vs. laser diffraction, Powder Technology, 177: 53-63.
43. ST Erdoğan, X Nie, PE Stutzman, EJ Garboczi (2010) Micrometer-scale 3-D imaging of eight cements: Particle shape, cement chemistry, and the effect of particle shape on laser diffraction size analysis, Cement and Concrete Research, 40: 731–739.
44. G Eshel, GJ Levy, U Mingelgrin, MJ Singer (2004) Critical Evaluation of the Use of Laser Diffraction for Particle-Size Distribution Analysis, SOIL SCI. SOC. AM. J., 68:736-743.
45. N Faria, MN Pons, S Feyo de Azevedo, FA Rocha, H Vivier (2003) Quantification of the morphology of sucrose crystals by image analysis, Powder Technology, 133: 54-67.
46. SP Friedman, DA Robinson (2002) Particle shape characterization using angle of repose measurements for predicting the effective permittivity and electrical conductivity of saturated granular media, WATER RESOURCES RESEARCH, VOL. 38, NO. 11, 1236, doi:10.1029/2001WR000746.
47. M Furuuchi, A Ikeuchi, T Fukagawa, K Gotoh (1988) Determination of particle shape from electrical conductivity of suspensions, Journal of Chemical Engineering of Japan. 21(5):528-533.
48. EJ Garboczi (2002) Three-dimensional mathematical analysis of particle shape using X-ray tomography and spherical harmonics: Application to aggregates used in concrete, Cement and Concrete Research, 32: 1621–1638.
49. EJ Garboczi (2011) Three Dimensional Shape Analysis of JSC-1A Simulated Lunar Regolith Particles, Powder Technology, 207: 96-103.
50. EJ Garboczi, JW Bullard (2013) Contact function, uniform-thickness shell volume, and convexity measure for 3D star-shaped random particles, Powder Technology, 237: 191-201.
51. EJ Garboczi, JW Bullard (2016) 3D analytical mathematical models of random star-shape particles via a combination of X-ray computed microtomography and spherical harmonic analysis, in Particle Shape Models, edited by T. Wriedt, Springer, 2016.
52. WA Gray (1968) The Packing of Solid Particles, Chapman & Hall, London.
53. D Gendzwill, M Stauffer (1981) Analysis of Triaxial Ellipsoids: Their Shapes, Plane Sections, and Plane Projections, Mathematical Geology, 13: 135-152.
54. RM German (1989) Particle Packing Characteristics. Metal Powder Industry. ISBN: 0918404835.
55. K Gotoh, JL Finney (1975) Representation of the size and shape of a single particle, Powder Technology, 12: 125-130.

56. K Gotoh, H Masuda, K Higashitani (1997) Powder Technology Handbook, 2nd Ed, Marcel Dekker.
57. DJ Graham and NG Midgley (2000) Graphical representation of particle shape using triangular diagrams: an Excel spreadsheet method, Earth Surf. Process. Landforms, 25, 1473–7.
58. M Grigoriu, EJ Garboczi, C Kafali (2006) Spherical harmonic-based random fields for aggregates used in concrete, Powder Technology, 166: 123-138.
59. Y Guo, JS Curtis (2015) Discrete element method simulations for complex granular flows, Annual Review of Fluid Mechanics, 47:21-46.
60. ML Hentschel, NW Page (2003) Selection of descriptors for particle shape characterization, Part. Part. Syst. Charact. 20:25-38.
61. GT Herman (2009) Fundamentals of computerized tomography: Image reconstruction from projection, 2nd edition, Springer.
62. H Heywood (1937) Numerical definitions of particle size and shape, Chem Ind. 15:149-154.
63. BR Jennings, K Parslow (1988) Particle size measurement: the equivalent spherical diameter, Proc. R. Soc. Lond. A 419:137-149.
64. X Jia, DJ Wedlock, RA Williams (2000) Simulation of simultaneous aggregation and sedimentation, Minerals Engineering, 13(13): 1349-1360.
65. X Jia, RA Williams (2001) A packing algorithm for particles of arbitrary shapes, Powder Technology, 120(3): 175-186.
66. X Jia, RA Williams (2007) A hybrid mesoscale modelling approach to dissolution of granules and tablets, Chemical Engineering Research & Design, 85(A7): 1027-1038.
67. X Jia, RA Williams, C Selomulya (2008) Three-dimensional measurement and simulation of the dewatering behaviour of flocs and sediments using X-ray microtomography, The Journal of The Southern African Institute of Mining and Metallurgy, 108: 1-6.
68. X Jia, R Caulkin, RA Williams, ZY Zhou, AB Yu (2010) The role of geometric constraints in random packing of non-spherical particles, Europhysics Letters, 92, 68005.
69. FW Jones (1938) The measurement of particle size by the X-ray method, Proceedings of the Royal Society of London, Series A, Mathematical and Physical Sciences, 166(924): 16-43.
70. A Laurentini (1997) How Many 2D Silhouettes Does It Take to Reconstruct a 3D Object? Computer Vision & Understanding, 67(1): 81–87.
71. Liang C, Wong KYK (2010) 3D reconstruction using silhouettes from unordered viewpoints, Image and Vision Computing, 28: 579–589.
72. IK Kazmi, L You, JJ Zhang (2013) A survey of 2D and 3D shape descriptors, Computer Graphics, Imaging and Visualization (CGIV), 2013 10th International Conference, 6-8 Aug 2013. pp.1-10. DOI: 10.1109/CGIV.2013.11.
73. D Karakuş, AH Onur, AH Deliormanlı, G Konak (2010) Size and shape analysis of mineral particles using image processing, The Journal of Ore Dressing, 12(23): 1-8.
74. BH Kaye, J Junkala, GG Clark (1998) Domain plotting as a technique for summarizing fineparticle shape, texture and size information, Part. Part. Syst. Charact., 15: 180–190.
75. BH Kaye (1978) Specification of the ruggedness and/or texture of a fine particle profile by its fractal dimension, Powder Technology, 21:1-16.
76. BH Kaye (1994) A Random Walk Through Fractal Dimensions, 2nd Ed, VCH Verlagsgesellschaft mbH, ISBN: 9783527290789.

77. BH Kaye (1997) Characterizing the flowability of a powder using the concepts of fractal geometry and chaos theory, Part. and Part. Syst. Charact., 14: 53-66.
78. BH Kaye (1999) Characterization of Powders and Aerosols, Wiley-VCH.
79. SG Kazarian, KLA Chan (2003) Chemical photography of drug release, Macromolecules, 36: 9866–9872.
80. SG Kazarian, AV Ewing (2013) Applications of Fourier transform infrared spectroscopic imaging to tablet dissolution and drug release, Expert Option on Drug Delivery, 10(9): 1207-1221.
81. I Kemelmacher-Shlizerman, R Basri (2011) 3d face reconstruction from a single image using a single reference face shape, IEEE Trans. Pattern Anal. Mach. Intell., 33(2): 394–405.
82. WC Krumbein (1934) Size frequency distributions of sediments. J. Sediment. Petrol., 4:65-77.
83. WC Krumbein (1941) Measurement and geological significance of shape and roundness of sedimentary particles, Journal of Sedimentary Petrology, 11(2): 64-72.
84. CY Kuo, JD Frost, JS Lai, LB Wang (1996) Three-dimensional image analysis of aggregate particles from orthogonal projections, Transportation Research Record 1526, National Research Council, Washington, DC, 1996, pp. 98-103.
85. C Lanczos (1956) Applied Analysis, Prentice Hall, Englewood Cliffs, NJ.
86. X Lin, TT Ng (1997) A three-dimensional discrete element model using arrays of ellipsoids. Geotechnique, 47(2): 319-329.
87. X Liu, EJ Garboczi, M Grigoriu, Y Lu, ST Erdoğan (2011) Spherical harmonic-based random fields based on real particle 3D data: Improved numerical algorithm and quantitative comparison to real particles, Powder Technology, 207: 78–86.
88. F Long, H Peng, E Myers (2007) Automatic segmentation of nuclei in 3D microscopy images of C.Elegans, in 2007 4th IEEE International Symposium on Biomedical Imagining: From Nano to Macro, 536-539.
89. H Ma, CA Anderson (2008) Characterization of pharmaceutical powder blends by NIR chemical imaging, Journal of Pharmaceutical Sciences, 97(8): 3306-3320.
90. Z Ma, HG Merkus, JGAE de Smet, C Heffels, B Scarlett (2000) New developments in particle characterization by laser diffraction: size and shape, Powder Technology, 111 (1-2): 66–78.
91. Z Ma, HG Merkus, B Scarlett (2001a) Extending laser diffraction for particle shape characterisation: technical aspects and application, Powder Technology, 118:180-7.
92. Z Ma, HG Merkus, HG van der Veen, M Wong, B Scarlett (2001b) On-line measurement of particle size and shape using laser diffraction, Part. Part. Syst. Charact., 18:243-7.
93. M Marigo, EH Stitt (2015) Discrete Element Method (DEM) for industrial applications: Comments on calibration and validation for the modelling of cylindrical pellets, KONA Powder and Particle Journal, 32: 236-252. Doi:10.14356/kona.2015016.
94. ML Hentschel, NW Page (2003) Selection of descriptors for particle shape characterization, Part. Part. Syst. Charact., 20(1): 25-38.
95. NJ McCormick, MG Gee (2005) The measurement of the shape of abrasive particles with confocal optical microscopy, NPL Report DEPC-MPE 010, February 2005. ISSN:1744-0262.
96. A Medalia (1970) Dynamic shape factors for particles, Powder Technology, 4: 117-138.
97. TP Meloy (1977a) A hypothesis for morphological characterization of particle shape and physiochemical properties, Powder Technology, 16: 233-253.

98. TP Meloy (1977b) Fast Fourier transforms applied to shape analysis of particle silhouettes to obtain morphological data, Powder Technology, 17: 27-35.
99. V Mikli, H Käerdi, P Kulu, M Besterci (2001) Characterization of Powder Particle Morphology, Proc. Estonian Acad. Sci. Eng., 7: 22-34.
100. M Miller, E Miller, J Liu, RM Lund, JP McKinley (2012) Microscale reconstruction of biogeochemical substrates using multimode X-ray tomography and scanning electron microscopy, American Geophysical Union, Fall Meeting 2012, abstract #V23C-2832.
101. OP Mills, WI Rose (2010) Shape and surface area measurements using scanning electron microscope stereo-pair images of volcanic ash particles, Geosphere, 6(6): 805-811. doi:10.1130/GES00558.1.
102. AA Mirghasemi, L Rothenburg, EL Matyas (2002) Influence of particle shape on engineering properties of assemblies of two-dimensional polygon-shaped particles, Geotechnique, 52, 209-217.
103. ME Möbius, BE Lauderdale, SR Nagel, HM Jaeger (2001) Brazil-nut effect: Size separation of granular particles, Nature, 414: 270. doi:10.1038/35104697.
104. CF Mora, AKH Kwan (2000) Sphericity, shape factor, and convexity measurement of coarse aggregate for concrete using digital image processing, Cement and Concrete Research, 30: 351-358.
105. R Moreno-Atanasio, RA Williams, X Jia (2010) Combining X-ray microtomography with computer simulation for analysis of granular and porous materials, Particuology, 8(2): 81-99.
106. H Mühlenweg, ED Hirleman (1998) Laser Diffraction Spectroscopy: Influence of Particle Shape and a Shape Adaptation Technique, Particle & Particle Systems Characterization, 15(4): 163–169.
107. F Müller, R Polke, M Schäfer, N Scholz (2001) Particle System Characterization and Modelling, Part. Part. Syst. Charact., 18, 248–253.
108. A Munjiza (2004) The Combined Finite-Discrete Element Method, Wiley, ISBN: 9780470841990.
109. A Munjiza, J Xiang, X Garcia, JP Latham, D Schiava, NWM John (2008) The Virtual Geoscience Workbench, VGW: Open Source Tools for Discontinuous Systems. Proceedings, Beijing DEM''08. 113-121.
110. M Naito, O Hayakawa, K Nakahira, H Mori, J Tsubaki (1998) Effect of particle shape on size distribution measured with commercial equipment, Powder Technology, 100:52-60.
111. NIST (2009) Glossary of Morphology Terms. http://www.nist.gov/lispix/doc/particle-form/part-morph-gloss.htm.
112. J Ollion, J Cochennec, F Loll, C Escudé, T Boudier (**2013**) TANGO: A Generic tool for high-throughput 3D image analysis for studying nuclear organization, Bioinformatics, 29(14):1840-1.
113. T Paik, BT Diroll, CR Kagan, CB Murray (2015) Binary and Ternary Superlattices Self-Assembled from Colloidal Nanodisks and Nanorods, Journal of the American Chemical Society, 137(20): 6662-6669.
114. MJ Pankhurst, KJ Dobson, DJ Morgan, SC Loughlin, TH Thordarson, PD Lee, L Courtois (2014) Monitoring the magmas fuelling volcanic eruptions in near-real-time using x-ray micro-computed tomography, Journal of Petrology, 55: 671-684. doi: 10.1093/petrology/egt079

115. AA Pena, PG Lind, HJ Herrmann (2008) Modeling slow deformation of polygonal particles using DEM, Particuology, 6:506-514.
116. AL Persson (1998) Image analysis of shape and size of fine aggregates, Engineering Geology, 50: 177-186.
117. G Pólya, G Szegő (1951) Isoperimetric inequalities in mathematical physics. No. 27. Princeton University Press.
118. MN Pons, H Vivier, J Dodds (1997) Particle shape characterization using morphological descriptors, Part. and Part. Syst. Charact., 14: 272-277.
119. MN Pons, H Vivier, T Rolland (1998) Pseudo-3D shape description for facetted materials, Part. Part. Syst. Charact., 15: 100-107.
120. MN Pons, H Vivier, K Belaroui, B Bernard-Michel, F Cordier (1999) Particle morphology: from visualisation to measurement, Powder Technology, 103: 44-57.
121. MN Pons, H Vivier, V Delcour, JR Authelin, L Pailleres-Hubert (2002) Morphological analysis of pharmaceutical powders, Powder Technology, 128(2-3): 276-286.
122. J-L Pouchou, D Boivin, P Beauchêne, G Le Besnerais, F Vignon (2002) 3D Reconstruction of Rough Surfaces by SEM Stereo Imaging, Microchimica Acta, 139(1):135-144.
123. P Pourghahramani, E Forssberg (2005) Review of applied particle shape descriptors and produced particle shapes in grinding environments. Part 1: Particle shape descriptors. Mineral Processing and Extractive Metallurgy Review, 26:2, 145-166, DOI: 10.1080/08827500590912095.
124. F Radjaï, F Dubois (2011) Discrete-element Modeling of Granular Materials, Wiley, New York.
125. PM Raj, WR Cannon (1999) 2-D particle shape averaging and comparison using Fourier descriptors, Powder Technology, 104: 180–9.
126. M Ramaioli (2008) Granular flow simulations and experiments for the food industry, PhD Thesis, THÈSE NO 3997 (2007), ÉCOLE POLYTECHNIQUE FÉDÉRALE DE LAUSANNE.
127. M. Ramaioli, L. Pournin and Th. M. Liebling (2005) Numerical and experimental investigation of alignment and segregation of vibrated granular media composed of rods and spheres, Powders and Grains 2005, II, 1359-1363, R. Garcia-Rojo, H. J. Herrmann and S. McNamara, A.A.Balkema Publishers.
128. DW Ritchie, GJL Kemp (1999) Fast computation, rotation, and comparison of low resolution spherical harmonic molecular surfaces, J. Comp. Chem., 20: 383–395.
129. N Roberts, D Magee, Y Song, K Brabazon, M Shires, D Crellin, P Quirke, D Treanor (2012) Toward Routine Use of 3D Histopathology as a Research Tool, Am. J. Pathol., 180:1835-1842.
130. DA Robinson, SP Friedman (2002) Observations of the effects of particle shape and particle size distribution on avalanching of granular media, Physica A, 311: 97–110.
131. JM Rodriguez, T Edeskär, S Knutsson (2013) Particle shape quantities and measurement techniques - A review, The Electronic Journal of Geotechnical Engineering, 18A:169-198.
132. S Roy, J Meunier, AM Marian, F Vidal, I Brunette, S Costantino (2012) Automatic 3D reconstruction of quasi-planar stereo Scanning Electron Microscopy (SEM) images, Conf Proc IEEE Eng Med Biol Soc., 2012:4361-4. doi: 10.1109/EMBC.2012.6346932.
133. JC Russ (1995) The Image Processing Handbook, 2nd Ed, CRC Press LLC, Boca Raton, Florida.

134. P Sacca (2015) GE's revolution CT scan shows amazing GIFs of the human body, Design & Trend, http://www.designntrend.com/articles/34445/20150112/ges-revolution-ct-scan-shows-amazing-gifs-human-body.htm.
135. KVS Sastry, H Cooper, RH Hogg, TLP Jespen, F Knoll, B Parekh, RK Rajamani, T Sorenson, I Wechsler (1997) Solid-Solid Operations and Equipment, in Perry RH and DW Green (eds), Perry's Chemical Engineers' Handbook, 7th Ed., McGraw-Hill, New York, 1997.
136. JC Santamarina, GC Cho (2004) Soil behaviour: the role of particle shape, Proc. Skempton Conf., March, London, 1-14.
137. DW Schaefer, JE Martin, P Wiltzius, DS Cannell (1984) , Fractal geometry of colloidal aggregates, Phys Rev Lett, 52(26): 2371-2374.
138. M Schäfer (2002) Digital Optics: Some Remarks on the Accuracy of Particle Image Analysis, Part. and Part. Syst. Charact., 19: 158-168.
139. HP Schwarcz, KC Shane (1969) Measurement of particle shape by Fourier analysis, Sedimentology, 13: 213-231.
140. J Seville, U Tüzun, R Clift (1997) Processing of Particulate Solids, Kluwer/Chapman & Hall, London.
141. KR Shah, SI Badawy, MM Szemraj, DB Gray, MA Hussain (2007) Assessment of segregation potential of powder belnds, Pharm Dev Technol, 12(5): 457-462.
142. WY Shih, J Liu, WH Shih, IA Aksay (1991) Aggregation of colloidal particles with finite interparticle attraction energy, Journal of Statistical Physics, 62(5/6): 961-984.
143. JA Slotwinski, EJ Garboczi, PE Stutzman, CF Ferraris, SS Watson, MA Peltz (2014), Characterization of Metal Powders Used for Additive Manufacturing, Journal of Research of the National Institute of Standards and Technology, Volume 119. http://dx.doi.org/10.6028/jres.119.018.
144. C DiStefano, V Ferro, S Mirabile (2010) Comparison between grain-size analyses using laser diffraction and sedimentation methods, Biosystems Eengineering, 106: 205-215.
145. PA Swanson, AF Vetter (1985) The measurement of abrasive particle shape and its effect on wear, A S L E Transactions, 28:2, 225-230, DOI: 10.1080/05698198508981615.
146. JWH Tangelder, RC Veltkamp (2008) A survey of content based 3D shape retrieval methods, Multimedia Tools and Applications, 39(3) 441-471.
147. AP Tinke, A Carnicer, R Govoreanu, G Scheltjens, L Lauwerysen, N Mertens, K Vanhoutte, ME Brewster (2008) Particle shape and orientation in laser diffraction and static image analysis size distribution analysis of micrometer sized rectangular particles, Powder Technology, 186: 154–167.
148. J Tsubaki, G Jimbo (1979a) A proposed new characterization of particle shape and its application, Powder Technology, 22: 161-169.
149. J Tsubaki, G Jimbo (1979b) The identification of particles using diagrams and distributions of shape indices, Powder Technology, 22: 171-178.
150. USP (2000) Optical Microscopy, General Test (776), USP 24, The US Pharmacopoeial Convention, Rockville, MD, (2000), pp.1965-1967.
151. JC Vickerman, IS Gilmore (2009) Surface Analysis - The Principal Techniques, 2nd Ed, Wiley. ISBN 978-0-470-01763-0.

152. GT Vickers (1996) The projected areas of ellipsoids and cylinders, Powder Technology, 86(2): 195–200.
153. A Videla, C-L Lin, JD Miller (2006) Watershed functions applied to a 3D image segmentation problem for the analysis of packed particle beds, Particle & Particle Systems Characterization, 23(3-4): 237–245.
154. DV Vranic, D Saupe (2001) 3D shape descriptor based on 3D Fourier transform, Proceedings of ECMCS-2001, the 3rd EURASIP Conference on Digital Signal Processing for Multimedia Communications and Services, 11 - 13 September 2001, Budapest, Hungary / ed. by Kálmán Fazekas. - Budapest : Scientific Assoc. of Infocommunications, 2001. - S. 271-274. - ISBN 963-8111-64-X.
155. H Wadell (1932) Volume, shape, and roundness of rock particles, J. Geol., 40:443–451.
156. H Wadell (1933) Sphericity and roundness of rock particles, J. Geol., 41:310-331.
157. H Wadell (1934) Shape determination of large sedimental rock fragments. The Pan-American Geologist, 61: 187-220.
158. H Wadell (1935) Volume, shape, and roundness of quartz particles, Journal of Geology, 43:250-279.
159. C Walther (2003) Comparison of colloid investigations by single particle analytical techniques—a case study on thorium-oxyhydroxides, Colloids and Surfaces A: Physicochemical and Engineering Aspects, 217(1-3): 81–92.
160. Y Wang, Y Wang, DR Breed, VN Manoharan, L Feng, AD Hollingsworth, M Weck, DJ Pine (2012) Colloids with valence and specific directional bonding, Nature 491:51–55.
161. WC Wentworth (1922) The shape of beach pebbles, Washington, U.S. Geological Survey Bulletin, 131C: 75-83.
162. WC Wentworth (1933) The shape of rock particle: A discussion, Journal of Geology, 41:306-309.
163. R Wettimuny, D Penumadu (2003) Automated digital image based measurement of boundary fractal dimension for complex nanoparticles, Part. Part. Syst. Charact., 20: 18-24.
164. T Whitmarsh, L Humbert, M De Craene, LM Del Rio Barquero, AF Frangi (2011) Reconstructing the 3D Shape and Bone Mineral Density Distribution of the Proximal Femur From Dual-Energy X-Ray Absorptiometry, IEEE TRANSACTIONS ON MEDICAL IMAGING, 30(12):2101-2114.
165. JC Williams (1976) The segregation of particulate materials. A review, Powder Technology, 15(2): 245-251.
166. RA Williams and X Jia (2003) Tomographic imaging of particulate systems, Advanced Powder Technology, 14(1): 1-16.
167. TA Witten, LM Sander (1981) Diffusion limited aggregation, a kinetic critical phenomenon, Phys Rev Lett, 47: 1400-1402.
168. R Xu, OA Di Guida (2003) Comparison of sizing small particles using different technologies, Powder Technology, 132(2–3): 145–153.
169. R Xu (2006) Particle Characterization: Light Scattering Methods, Kluwer Academic Publishers. ISBN: 0792363000.
170. L Yang, F Albregtsen, T Lonnestad, P Grottum (1994) Methods to estimate areas and perimeters of blob-like objects: A comparison, MVA'94 IAPR Workshop on Machine Vision Applications, Dec 13-15, 1994, Kawasaki.

171. BD Young, AW Bryson, BM Van Vliet (1990) An evaluation of the technique of polygonal harmonics for the characterisation of particle shape, Powder Technology, 63: 157-168.
172. M Zeidan, X Jia, RA Williams (2007) Errors Implicit in digital particle characterisation, Chemical Engineering Science, 62(7): 1905-1914.
173. D Zhang, D Lu (2004) Review of shape representation and description techniques, Pattern Recognition, 37: 1-19.
174. H Zhu Z Zhou, RY Yang, AB Yu (2007) Discrete particle simulation of particulate systems: theoretical developments. Chem. Eng. Sci. 62:3378–3396.
175. H Zhu, Z Zhou, RY Yang, AB Yu (2008) Discrete particle simulation of particulate systems: a review of major applications and findings. Chem. Eng. Sci. 63:5728–5770.

Figure 1. Illustration of shape segregation experiments involving iso-volume particles of three different shapes (a) S-SS mixture, (b) SS-LS mixture and (c) S-LS mixture. The trend is somewhat unexpected of a typical Brazil nut effect, demonstrating the importance of particle shape for a predominantly size effect. [Images generated by DigiPac for illustration under the conditions used in the experiments by Ramaioli (2008)]

Figure 2: Example of a 3D object and its 2D projections.

Figure 3: (a) Calculated diffraction pattern of a circle and a square. (b) SEM photos of powdered glass and a single ash particle from volcanic eruption. [Source: (a) from Fig.1 in Ma et al (2000); (b) from http://www.scielo.br/img/fbpe/ce/v44n289/n289a2f1.gif and http://volcanoes.usgs.gov/Imgs/Jpg/Tephra/SarnaSem_60-010_large.jpg]

Figure 4 CT scan examples where shape extraction is required for (a) digitisation or (b) orientation distribution.

Figure 5 Harmonic and Fourier analysis examples.

Figure 6: (a) 3D VRML (Virtual Reality Modeling Language) images from eight different cements (Erdoğan et al, 2010). (b) A gravel particle showing both the voxelated image measured by X-ray CT and the spherical harmonic generated VRML image of the same piece of gravel (Garboczi, 2002).

Table 1: Comparison between shape representations typically used in particle simulations

	Parametric	Mesh based	Sphere-composite	Image based
Description	Spheres defined by centre and radius; ellipsoids defined by centre and principal dimensions; rocks defined by spherical harmonics (Garboczi, 2002)	Mesh over the surface of an object	Primary sphere, sometimes of very different sizes, are clumped together to form a shape.	Shapes are represented and treated as digital images (Jia and Williams, 2001).
Use	Discrete Element Models (Zhu et al, 2007 and 2008; Lin and Ng, 1997) and DEM programs	Computer graphics, commercial CAE packages, and DEM software (Munjiza, 2004; Munjiza et al, 2008; Pena et al, 2008)	Particle-level simulations of simple shapes (Moreno-Atanasio et al, 2010; Guo and Curtis, 2015)	Lattice based DEM and Monte Carlo models for arbitrary shapes and computer games
Pros	Memory efficient. Amenable to analytical analysis. Precise computational geometry. Easy to morphing into similar shapes for trend analysis.	Well established in computer graphics/games industry. Large user base for CAE as well. Easier to simulate deformable particles .	Easily assembled and broken as required. Relatively easy to implement.	Easy and straightforward to implement software. Efficiency increases with shape complexity. Details are captured at voxel level, thus better suited for simulations of conductivity etc. Easily assembled, deformed or broken in principle at least.
Cons	Difficult to develop robust and efficient code for collision/overlap detection, least popular for particle-level simulations.	Difficult to break at arbitrary points/planes. Difficult to develop robust and efficient code for collision/overlap detection, least popular for particle-level simulations.	Can change the nature of contacts (from face/line contacts to point contacts); require calibrations by trial-and-error to set parameters (Marigo and Stitt, 2015); results can be sensitive to shape make-up (Caulkin et al, 2015).	Memory intensive; simpler shapes do not mean less memory; artificial surface roughness always exist; results can be sensitive to resolution.

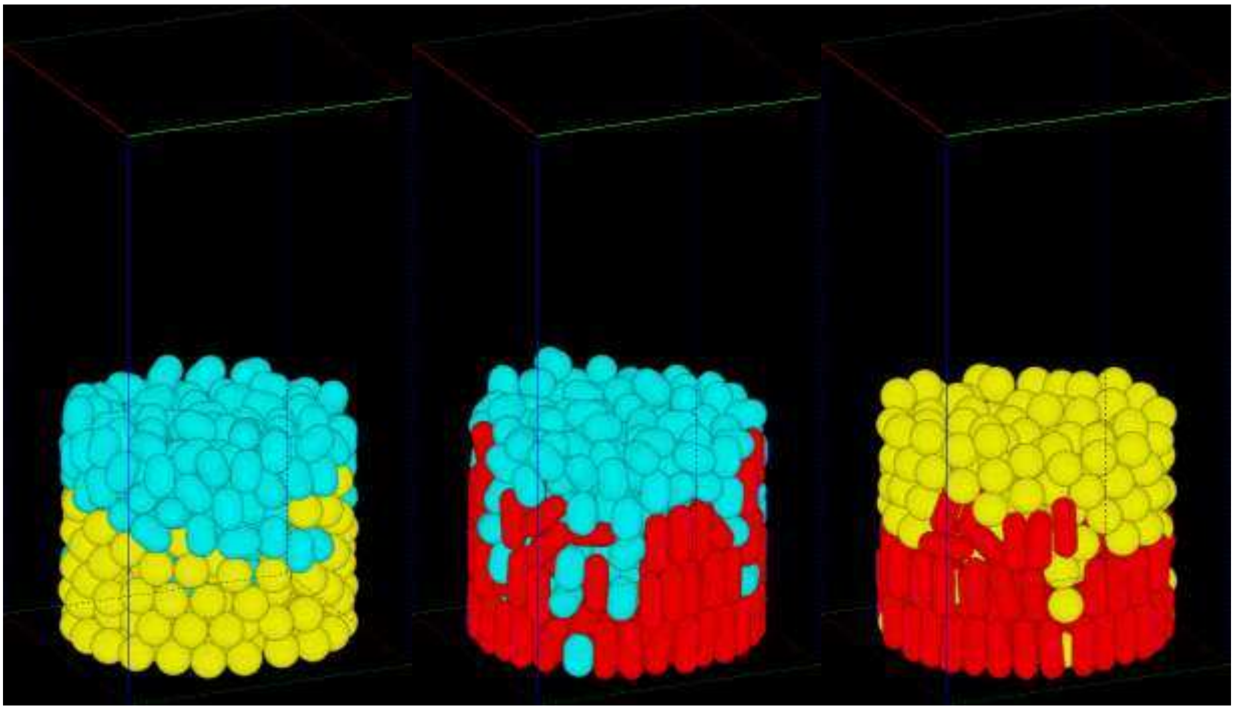

Fig.1

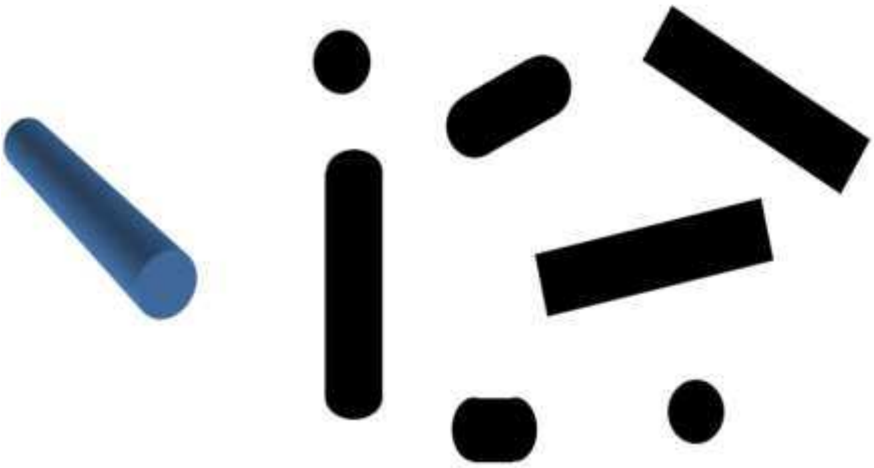

Fig.2

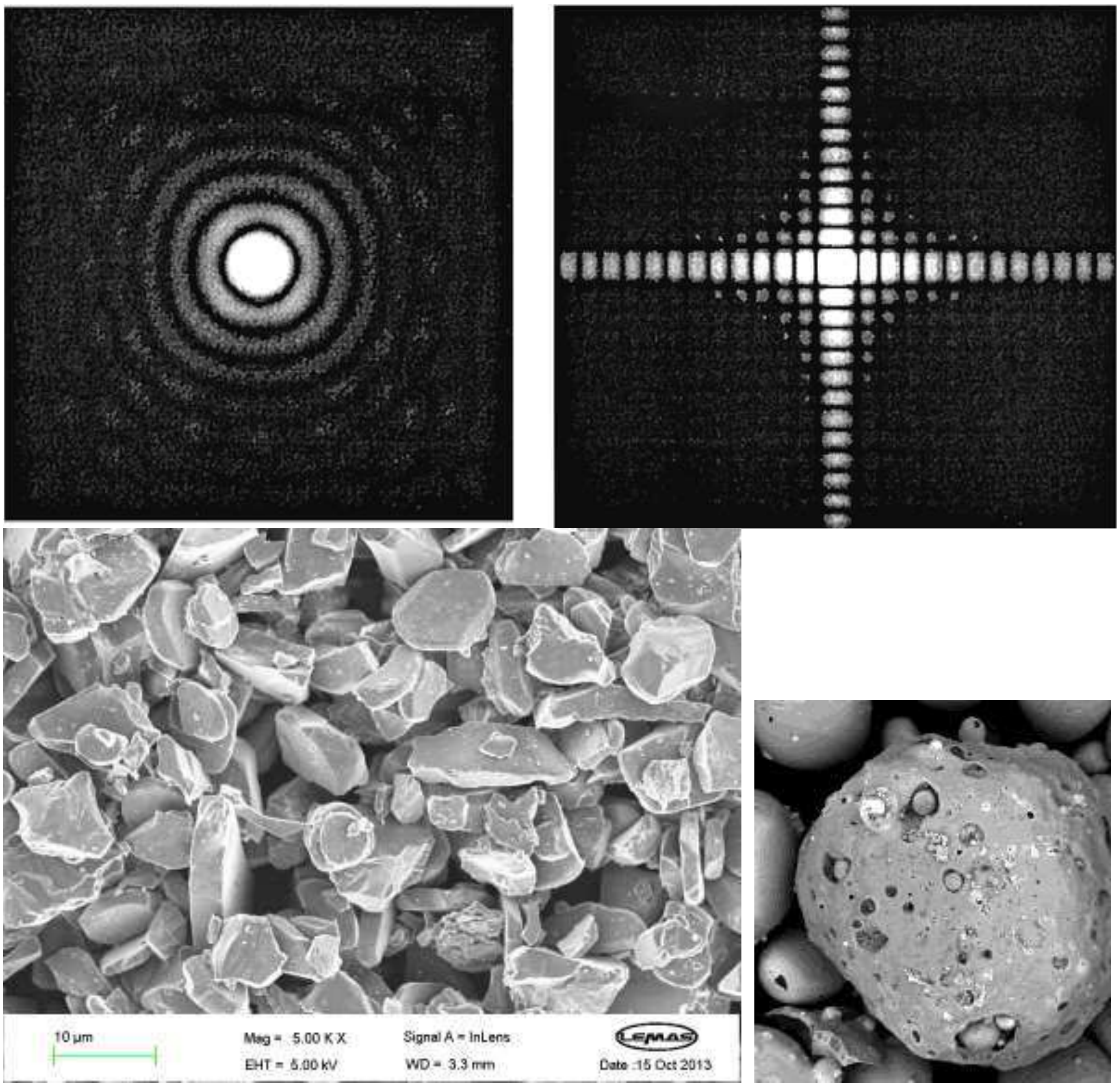
10 µm
Mag = 5.00 K X
EHT = 5.00 kV
Signal A = InLens
WD = 3.3 mm
LEMAS
Date :15 Oct 2013

Fig.3

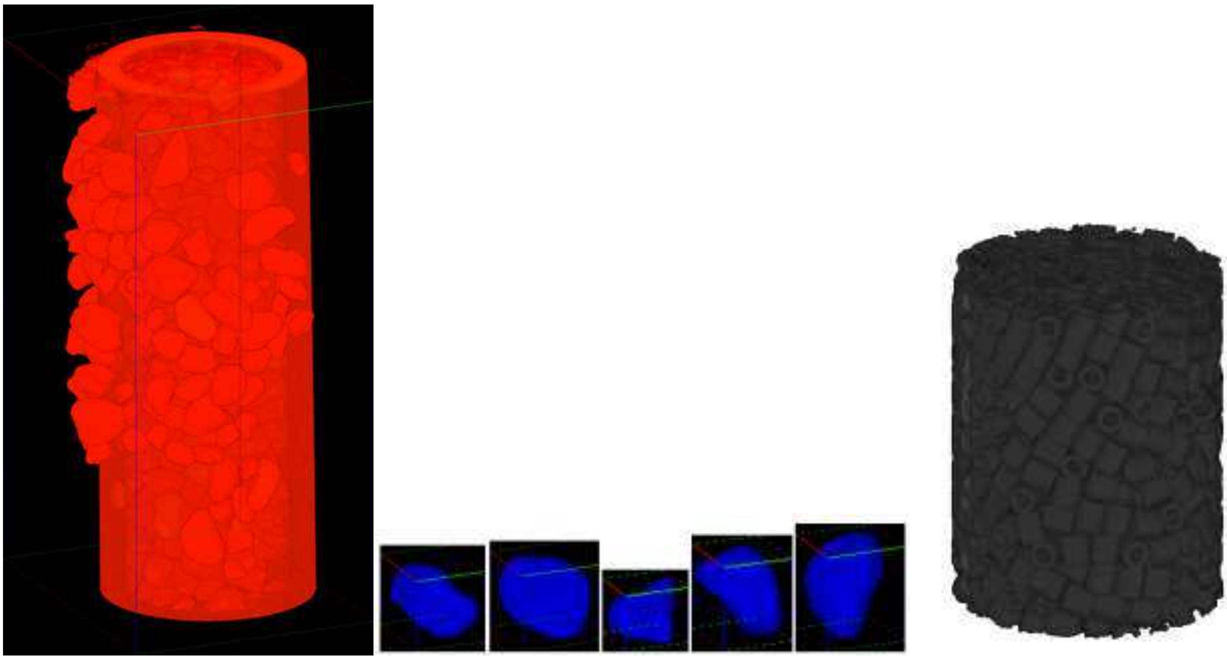

Fig.4

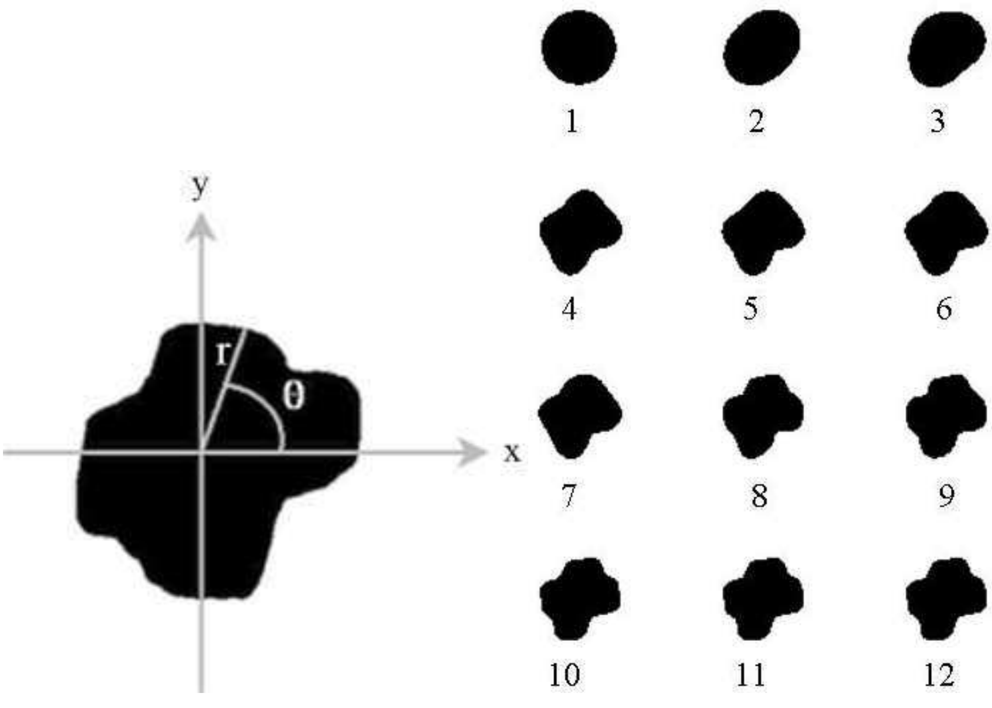

Fig.5

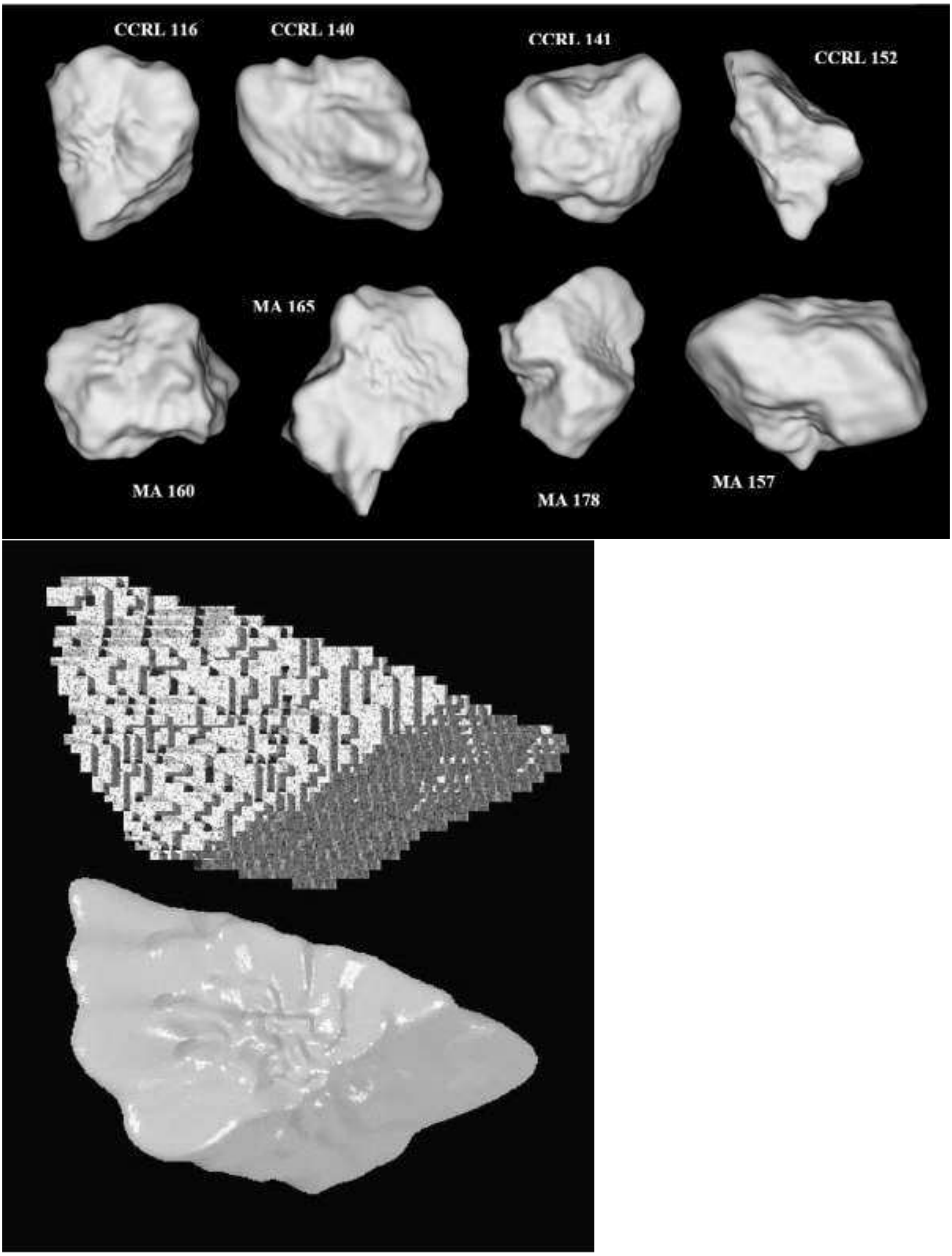

Fig.6